Bone 49 (2011) 790–798

Contents lists available at ScienceDirect

Bone

journal homepage: www.elsevier.com/locate/bone

α-Actinin-3 deficiency is associated with reduced bone mass in human and mouse

Nan Yang [a,b,*], Aaron Schindeler [b,c], Michelle M. McDonald [c], Jane T. Seto [a,b], Peter J. Houweling [a], Monkol Lek [a,b], Marshall Hogarth [a,b], Alyson R. Morse [c], Joanna M. Raftery [a], Dominic Balasuriya [a], Daniel G. MacArthur [d], Yemima Berman [a,b], Kate GR Quinlan [a,b], John A. Eisman [e], Tuan V. Nguyen [e], Jacqueline R. Center [e], Richard L. Prince [f,g], Scott G. Wilson [f,g], Kathy Zhu [f,g], David G. Little [b,c], Kathryn N. North [a,b,*]

[a] Institute for Neuroscience and Muscle Research, The Children's Hospital at Westmead, Sydney 2145, NSW, Australia
[b] Discipline of Paediatrics and Child Health, Faculty of Medicine, University of Sydney, Sydney 2006, NSW, Australia
[c] Orthopaedic Research Unit, The Children's Hospital at Westmead, Sydney 2145, NSW, Australia
[d] Wellcome Trust Sanger Institute, Hinxton, CB10 1SA, UK
[e] Osteoporosis and Bone Biology, Garvan Institute of Medical Research, St Vincent's Hospital and UNSW, Sydney, NSW 2010, Australia
[f] School of Medicine and Pharmacology, University of Western Australia, Perth 6009, WA, Australia
[g] Department of Endocrinology and Diabetes, Sir Charles Gairdner Hospital, Perth 6009, WA, Australia

ARTICLE INFO

Article history:
Received 12 November 2010
Revised 28 June 2011
Accepted 7 July 2011
Available online 19 July 2011

Edited by: R. Baron

Keywords:
ACTN3
R577X
Bone mass
BMD

ABSTRACT

Bone mineral density (BMD) is a complex trait that is the single best predictor of the risk of osteoporotic fractures. Candidate gene and genome-wide association studies have identified genetic variations in approximately 30 genetic loci associated with BMD variation in humans. α-Actinin-3 (*ACTN3*) is highly expressed in fast skeletal muscle fibres. There is a common null-polymorphism R577X in human *ACTN3* that results in complete deficiency of the α-actinin-3 protein in approximately 20% of Eurasians. Absence of α-actinin-3 does not cause any disease phenotypes in muscle because of compensation by α-actinin-2. However, α-actinin-3 deficiency has been shown to be detrimental to athletic sprint/power performance. In this report we reveal additional functions for α-actinin-3 in bone. α-Actinin-3 but not α-actinin-2 is expressed in osteoblasts. The *Actn3*$^{-/-}$ mouse displays significantly reduced bone mass, with reduced cortical bone volume (−14%) and trabecular number (−61%) seen by microCT. Dynamic histomorphometry indicated this was due to a reduction in bone formation. In a cohort of postmenopausal Australian women, *ACTN3* 577XX genotype was associated with lower BMD in an additive genetic model, with the R577X genotype contributing 1.1% of the variance in BMD. Microarray analysis of cultured osteoprogenitors from *Actn3*$^{-/-}$ mice showed alterations in expression of several genes regulating bone mass and osteoblast/osteoclast activity, including *Enpp*1, *Opg* and *Wnt*7b. Our studies suggest that *ACTN3* likely contributes to the regulation of bone mass through alterations in bone turnover. Given the high frequency of R577X in the general population, the potential role of *ACTN3* R577X as a factor influencing variations in BMD in elderly humans warrants further study.

© 2011 Elsevier Inc. All rights reserved.

Introduction

Fragility fractures associated with declining bone mineral density (BMD) in osteoporosis represent a major cause of morbidity in humans [1]. Osteoporosis is a common disease affecting both sexes that increases in prevalence as people age, especially as women pass through menopause [2]. A combination of genetic factors, age, disease status, and body weight are the major determinants to the BMD variations seen in humans [3–7]. Three recent genome-wide association (GWA) studies [8–10] and one meta-analysis [11] in large cohorts of European-descent have revealed almost 30 loci associated with BMD, including *LDL receptor-related protein 5 (LRP5)*, *Osteoprotegerin (OPG)*, *Receptor Activator of Nuclear factor Kappa B (RANK)*, and its ligand *RANKL*. These proteins belong to the bone-forming (Wnt-β-catenin signalling [12]) and the bone-resorbing (RANK-RANKL-OPG [13]) pathways respectively through which they play key roles in the regulation of bone mass and remodelling. Mutations or alterations in these key pathways result in clinical manifestations of altered bone mass and disease. However, gene associations with BMD defined so far explain only a small percentage of the variance (less than 5%) and a substantial portion of the genetic variance of BMD remains unexplained. Over the past decade, candidate gene association studies have shown that the approach is still a valid method for in-depth analysis [14].

The α-actinins are a family of spectrin-like actin-binding proteins that consists of four members with critical roles in cytoskeleton maintenance and muscle contraction [15]. Two muscle isoforms, α-actinin-2 (*ACTN2*)

* Corresponding authors at: Institute for Neuroscience and Muscle Research, The Children's Hospital at Westmead, Locked Bag 4001, Westmead, Sydney, NSW 2145, Australia. Fax: +61 298453389.
E-mail addresses: nan.yang@persongen.com (N. Yang), Kathryn@chw.edu.au (K.N. North).

8756-3282/$ – see front matter © 2011 Elsevier Inc. All rights reserved.
doi:10.1016/j.bone.2011.07.009

and α-actinin-3 (*ACTN*3) are structurally similar but possess different patterns of expression; *ACTN*2 is expressed in all skeletal muscle fibres in cardiac muscle and the brain [16]. The expression of *ACTN3* was initially reported to be restricted to fast skeletal muscle fibres [16], however we subsequently identified low levels of expression in brain [17]. In contrast, the non-muscle isoforms (α-actinin-1 and -4) are broadly expressed in a range of cell and tissue types [15,16].

The common null R577X polymorphism in the *ACTN3* gene converts the codon for arginine (R) at position 577 to a premature stop codon (X), resulting in complete deficiency of α-actinin-3 in homozygote humans (*ACTN3* 577XX-genotype) [17]. The frequencies of the 577XX (α-actinin-3 deficient) genotype differ in human populations ranging from ~1% in East Africans, to ~20% in Europeans and up to ~25% in East Asians [18,19]. α-Actinin-3 deficiency does not result in a disease phenotype, suggesting that α-actinin-3 is not essential for muscle development or normal cell function, and that α-actinin-2 is able to provide functional compensation at least in fast muscle fibres [18]. Intriguingly, α-actinin-3 deficiency is detrimental to sprint and power performance in elite athletes [20] and in the general population [21], but is potentially beneficial to endurance performance [20]. This suggests that α-actinin-3 influences fast muscle fibre function at extreme levels of performance such that α-actinin-2 cannot compensate completely.

We have generated an α-actinin-3 knockout (*Actn3*$^{-/-}$) mouse model that mimics α-actinin-3 deficiency in humans. In this mouse model, loss of α-actinin-3 results in a shift in muscle metabolism towards the more efficient aerobic pathway [22], a shift in the properties of fast fibres towards those characteristic of slow fibres [23,24], and an increase in glycogen content in *Actn3*$^{-/-}$ mouse muscle associated with alteration in the activity of glycogen phosphorylase, which interacts directly with sarcomeric α-actinins [25]. All of these findings are consistent with human data and provide an explanation for previous human association studies, i.e. the slower muscle phenotype associated with α-actinin-3 deficiency would be detrimental to sprint performance and advantageous for endurance performance. Despite a small reduction in total body weight (~4%) in *Actn3*$^{-/-}$ mice compared to wild-type (WT), all *Actn3*$^{-/-}$ muscles containing fast 2B fibres exhibit a significantly reduced fibre size (~30%) and reduced muscle mass (10–20%) compared to muscles from WT littermates [24]. A recent human association study demonstrated that α-actinin-3 deficient women (*ACTN3* 577XX-genotype) have significantly reduced fat-free mass compared to RR or RX women who express α-actinin-3 [26]. Postmenopausal *ACTN3* 577XX women were also found to have reduced cross sectional area (fibre size) in their thigh muscles [27]. These studies suggest a role for α-actinin-3 in regulating muscle mass and fibre size.

The non-muscle α-actinins are expressed in both osteoblasts and osteocytes where they play two major roles. Within the cytoskeleton, α-actinin contributes to cell morphology [28] and stiffness [29] allowing adaptation to varied mechanical loads [30]. At focal adhesions, α-actinin interacts with integrin and focal adhesion kinase which contributes to the regulation of cell survival [31,32]. In this study, we show in addition to the non-muscle α-actinins, α-actinin-3 is also expressed in osteoblasts. Thus, given the presence of α-actinins in bone cells, the loss of α-actinin-3 may contribute to various bone phenotypes. Using our *Actn3*$^{-/-}$ mouse we explore the effects of α-actinin-3 deficiency on whole body bone mineral density (BMD), trabecular and cortical bone mass and architecture, bone formation and primary bone precursor cell phenotype. In our two post-menopausal women cohorts, we analyse the contribution of the *ACTN3* R577X polymorphism on BMD variation.

Materials and methods

The animal study was approved by our local Animal care and Ethics Committee. All tests were performed on either the R129 or C57BL6 genetic background. Mice were provided food and water *ad libitum*, and maintained on a 12:12 h cycle of light and dark. Human genetic association studies, CAIFOS (University of Western Australia Ethics Committee, Perth, Australia) and DOES (St. Vincent's Hospital Research Ethics Committee, Sydney, Australia) were approved by their local human ethics committees respectively.

DEXA analysis

Whole animals were placed in a GE Lunar Piximus2 (Lunar, Madison, WI) Dual Energy X-ray Absorptiometry (DEXA) scanner. The DEXA was calibrated using a hydroxyapatite "phantom" mouse model provided by the supplier. Data analysis was performed using the supplier's software with default settings. Bone mineral density (BMD; g/cm^2) was calculated using the mouse body and limbs, excluding the head and tail.

Isolation of mouse femurs

Femurs were removed from culled mice and stripped of excess soft tissue. Samples were then fixed in phosphate buffered 4% paraformaldehyde at room temperature for 24 h before being transferred to 70% ethanol at 4 °C for storage.

Q-CT analysis

Left femurs were placed into a plastic tube with 70% ethanol. The plastic tube was positioned in a XCT-960A scanner (STRATEC NORLAND) for quantitative computed tomography (Q-CT) analysis. The entire femur was scanned at a scan resolution of 70 μm and a slice thickness of 0.5 mm. The mean value of bone mineral content (BMC) was compared in each scanned section along the entire length of the bones.

Micro-CT analysis

Femurs stored at 70% ethanol were re-hydrated in saline for 48 h before being placed in a tube filled with saline and the distal half of the femurs scanned using a Skyscan 1174 MicroCT scanner (Skyscan, Belgium) at a resolution of 9.4 μm using a 0.5 mm Aluminium filter. Reconstruction of scans was done using a threshold of 0.09 and samples analysed using Skyscan CtAn software. Regions of interest were selected for trabecular bone in the distal metaphysis and cortical bone in the mid diaphysis and data generated for bone volume (BV), trabecular number (TbN), trabecular thickness (TbTh) and cortical thickness (CrtTh).

Histological analysis of distal femora

Mice were administered calcein at 10 mg/kg by subcutaneous injection 10 and 3 days prior to cull at 2 months of age to allow for analysis of dynamic bone formation parameters.

After CT analysis the distal femurs were processed to resin and 5 μm thick sections were cut from the sagittal plane in the centre of the lateral condyle. Sections were cleared of resin for analysis of calcein labels for dynamic bone formation parameters. In addition sections were stained by von Kossa for mineralised tissue to measure bone surface and for tartrate-resistant acid phosphatase (TRAP) to measure osteoclast number and surface.

Osteoblast cell culture and analysis

Primary human bone cells were isolated from an iliac crest bone biopsy from a 14 year old female with *ACTN3* RX genotype (expressing α-actinin-3 protein) (human ethics approval #2007/013). Primary mouse bone marrow stromal cells (BMSCs) were isolated from WT and *Actn3*$^{-/-}$ mice and cultured by adherence plating to tissue culture plastic. The mouse MC3T3-E1 pre-osteoblastic cell line was also used. Human and mouse primary cells were initially grown in DMEM containing 10% FBS and, when passaged, cells were replated at a standard density of 3.5×10^3 cells/cm^2. Mouse and human osteoprogenitors were differentiated in α-MEM

Table 1
ANOVA of female BMD and *ACTN3* R577X in CAIFOS cohort.

Groups	Response	Predictor	F value	Pr (>F)
CAIFOS (Perth)				
WB-BMD (n = 733)	WB-BMD	ACTN3 R577X	9.07	**0.003**
		Age	0.017	0.84
		BMI	0.454	0.50

WB-BMD: Whole body BMD.

containing 10% FBS supplemented with 50 μg/ml ascorbic acid and 10 mM β-glycerophosphate. To further stimulate osteogenic differentiation, select wells of primary mouse BMSCs were further stimulated with 300 ng/ml recombinant human bone morphogenetic protein-2 (rhBMP-2).

Primary human bone cells and MC3T3-E1 cells were used for immunohistochemistry (IHC) analysis using actinin1 to 4 specific antibodies. Primary mouse BMSCs were examined in cell viability, growth, and osteoblast differentiation. Cell viability was tested using the One Solution Cell Proliferation Assay Reagent (Promega). Cell growth was tested using a ^{3}H-thymidine incorporation assay. Cell differentiation was examined using alkaline phosphatase staining. Primary mouse BMSCs were also used for RNA isolation for microarray studies and qPCR analysis.

Immunohistochemistry analysis

Cells were fixed with 4% PFA containing 0.1% saponin on glass cover slips. After blocking with 2% BSA for 10 min, primary antibodies against α-actinin-1, -2, -3 and -4 (kindly provided by Dr Alan Beggs, Boston USA) were applied to the cells. After incubation for 1 h, the slides were washed twice with 1× PBS and re-blocked with 2% BSA for 10 min prior to incubation with Cy3-conjugated anti-rabbit IgG secondary antibody (1:250 dilution; Jackson ImmunoResearch) for 1 h at room temperature. All samples were washed twice with 1× PBS. All images were captured using ProgRes camera and software (SciTech).

Total RNA isolation for analysis of microarray, RT-PCR and q-PCR

Primary osteoblast cell were washed once with 1× PBS, and lysed with 1 ml of Tri-Reagent (Molecular Research Center) and total RNA was extracted as per manufactures conditions. Briefly, the lysates were transferred to a 2-ml Eppendorf tube and 0.2 ml of chloroform was added. The homogenate was vortexed for 1 min and then centrifuged at 12,000 *g* for 15 min at 2–8 °C. The upper aqueous solution was transferred to a fresh tube, and total RNA was precipitated with 0.5 ml of isopropyl alcohol per 1 ml of Tri-Reagent used in the initial lysate. The RNA was pelleted by centrifugation at 12,000 *g* for 10 min and washed with 1 ml of 70% ethanol, the RNA pellet was dissolved in 0.35 ml of RLT buffer from RNeasy Mini Kit (Qiagen). Further purification of total RNA was achieved using the RNeasy Mini Kit (Qiagen) following the manufacturer's instruction. The quality of RNA was analysed using the Agilent RNA BioAnalyzer and RNA Nano chip (Agilent Technologies).

For microarray analysis, aRNA was prepared using an aRNA amplification kit (Ambion) and Illumina mouse whole-genome bead-chips (Version2) following manufactures instructions. Differentially expressed genes were analysed using supplied BeadsStudio software, followed by validation by quantitative PCR (q-PCR) with TaqMan probes (Applied Biosystems). For reverse transcriptase PCR (RT-PCR) and q-PCR analysis, cDNA was synthesised using SuperScript III (Invitrogen) and random primers (Roche). Gene specific primers were designed and ordered from Sigma-Aldrich.

Statistical analysis of DOES and CAIFOS cohorts

For each dataset, individuals with missing age, BMI, BMD and genotype values were filtered out. The R Statistical Environment was used to perform regression analysis on this filtered dataset, using *ACTN3* R577X genotype, age and BMI as predictors (i.e. independent variables) and BMD as the response (i.e. dependent variable). The results of the univariate ANOVA, including sequential F tests are reported in Table 1.

Statistical analysis of animal samples

Independent samples Mann Whitney U tests were used for DEXA, QCT, μCT and histological outcomes with significance at $p<0.05$.

Results

Bone mass is reduced in Actn3$^{-/-}$ mice

In order to further characterise the changes on whole body composition in the context of α-actinin-3 deficiency, we performed the DEXA (dual-energy X-ray absorptiometry) scans on >160 mice (*Actn3*$^{-/-}$ mice n = 86, WT littermates n = 79). We observed that bone mineral density (BMD) (g/cm^2) was significantly reduced in *Actn3*$^{-/-}$ mice (Fig. 1), while *Actn3*$^{+/-}$ mice have an intermediate phenotype (Fig. S2). Since we have previously reported a decrease in lean mass as well as lower quadriceps muscle mass in *Actn3*$^{-/-}$ mice [24] and α-actinin-3 had only been previously implicated in fast muscle fibre function, we considered the possibility that the lower BMD was secondary to the muscle phenotype. However, the muscle mass difference between WT and *Actn3*$^{-/-}$ mice is lost after 4 months of age in male mice [33], suggesting that lower bone mass in *Actn3*$^{-/-}$

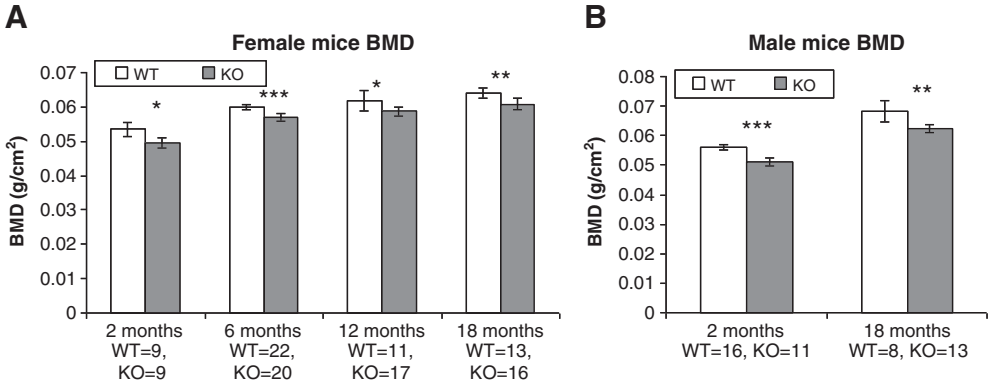

Fig. 1. Mouse whole body BMD determined using dual-energy X-ray absorptiometry (DEXA). The mean BMD (with 95% CI) in *Actn3*$^{-/-}$ mice was significantly lower than that in wild-type (WT) litter mates in female (1A) and male (1B) mice, across all analysed age groups. (*: $p<0.05$; **: $p<0.01$; ***: $p<0.001$). The average reduction of BMD in 2 month and 18 month old male mice was 9%, and the average reduction of BMD was 9% in 2 month old female *Actn3*$^{-/-}$ mice and 5% in older female *Actn3*$^{-/-}$ mice (6 month, 12 month and 18 month).

may be independent of lower muscle mass. On this basis, we performed a more detailed study in mice of different ages and genders and confirmed a consistent and significant reduction of BMD associated with α-actinin-3 deficiency, with a 9% reduction of BMD in all male *Actn3*$^{-/-}$ mice (2 month and 18 month old) (Fig. 1B), a 9% reduction in 2 month old female *Actn3*$^{-/-}$ mice, and a 5% reduction in older female *Actn3*$^{-/-}$ mice (6 month, 12 month and 18 month old) (Fig. 1A). In older male age groups, the reduction in BMD occurs in the absence of differences in muscle mass.

To obtain additional data regarding bone structure, femurs isolated from 6 month old female mice were fixed in 4% PFA and scanned by a Stratec XCT-960A scanner for quantitative computed tomography (Q-CT) analysis. The mean value of bone mineral content (BMC) was compared in each scanned section along the entire length of the femurs. Total BMC was significantly lower in *Actn3*$^{-/-}$ mice compared to WT mice, with an average reduction of 6–9% along the length of the femur ($p<0.01$–0.001) (Fig. 2A). Femurs isolated from 2 month old male mice were also Q-CT scanned and showed reductions in total BMC of 14–20% along the length of the femur in *Actn3*$^{-/-}$ mice compared to WT ($p<0.01$–0.001) (Fig. 2B). These Q-CT scans confirmed initial observation from DEXA that *Actn3*$^{-/-}$ mice have reduced bone mass.

Distal femurs from 2 month old male *Actn3*$^{-/-}$ and WT mice were scanned at high resolution to examine changes in cortical and trabecular bone volume (BV) relative to total volume (TV), using a Skyscan 1172 micro-CT (μCT). Compared to WT, *Actn3*$^{-/-}$ mice demonstrated a 59% reduction in trabecular bone volume (BV) *vs.* total bone volume (TV) ($p<0.01$) (Fig. 3A) and a 14% reduction in cortical bone volume ($p<0.01$) (Fig. 4A). As a result of these losses in bone tissue mass, both cortical and trabecular bone architecture was compromised. Both cortical thickness (Figs. 4B and C) and trabecular bone thickness (Fig. 3B) were reduced by 7% in *Actn3*$^{-/-}$ mice compared to WT ($p<0.05$), and the number of trabeculae was reduced by 61% in *Actn3*$^{-/-}$ mice compared to WT ($p<0.01$) (Fig. 3C). Such decreases in long bone structural mass, especially the large reduction in the number of bone trabeculae in *Actn3*$^{-/-}$ mice as illustrated in the 3-Dimensional μCT image (Fig. 3D), may reduce the resistance of these bones to fracture.

Detailed analysis of bone formation parameters on histological sections of distal femora from 2 month old mice confirmed the reduced bone mass was a direct result of impaired bone formation. Mineral apposition rate (MAR) on trabecular bone surfaces was significantly reduced by 20% in *Actn3*$^{-/-}$ compared to WT ($p<0.01$) (Figs. 5A and D). Further, bone formation rate per unit bone surface (BFR/BS) was reduced by 21% in *Actn3*$^{-/-}$ compared to WT ($p<0.05$, Fig. 5B). Mineralising surface (MS) was not significantly altered in *Actn3*$^{-/-}$ mice. Further, osteoclast number per unit bone surface (OscN/BS) on trabecular bone was increased by 24% in *Actn3*$^{-/-}$ mice compared to WT however this did not reach significance ($p=0.062$, Fig. 5C).

α-Actinin-3 is expressed in osteoprogenitor cells

DEXA, CT and histological data strongly suggest that, in addition to effects on muscle mass and fibre size, α-actinin-3 is involved in regulating bone mass and osteogenesis. In order to further investigate any potential direct effects on bone, the expression and activity of α-actinin-3 and the other α-actinins were examined in cultured bone marrow osteoprogenitors.

Immunohistochemistry (IHC) analysis for expression of α-actinin-1, -2, -3 and -4 was performed on human primary bone marrow stromal cells (isolated from a 14 year old female with *ACTN3* RX genotype-expressing α-actinin-3 protein) and murine MC3T3-E1 pre-osteoblastic

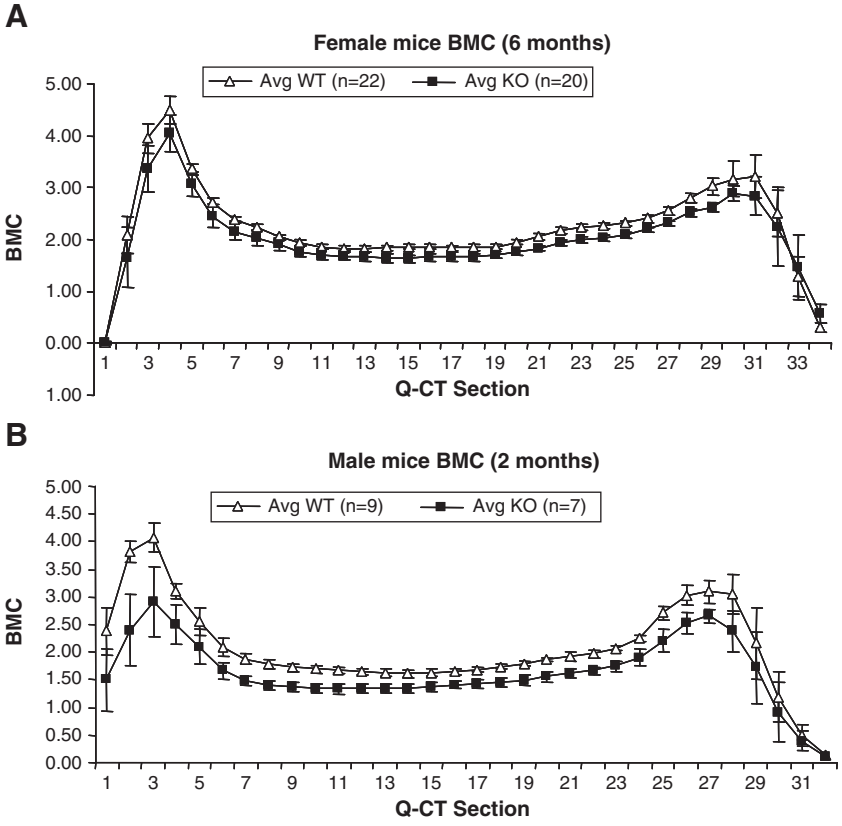

Fig. 2. Mouse BMC determined using Q-CT scan on isolated right femurs. Femurs were collected from 6 month old female mice (2A) and 2 month old male mice (2B). Entire femur was scanned with 0.5 mm width per section, and BMC values were collected from each section. *P* value was calculated by Mann Whitney *U*-test with 95% CI. The mean BMC at each corresponding section in 6 month old female (sections 5–30) and 2 month old male (sections 5–28), *Actn3*$^{-/-}$ mice were significantly lower than that in WT litter mates ($p<0.01$–0.001). The average reduction of BMC in 6 month old female *Actn3*$^{-/-}$ mice was 6–9%, and the average reduction of BMC in 2 month old male *Actn3*$^{-/-}$ mice was 14–20%.

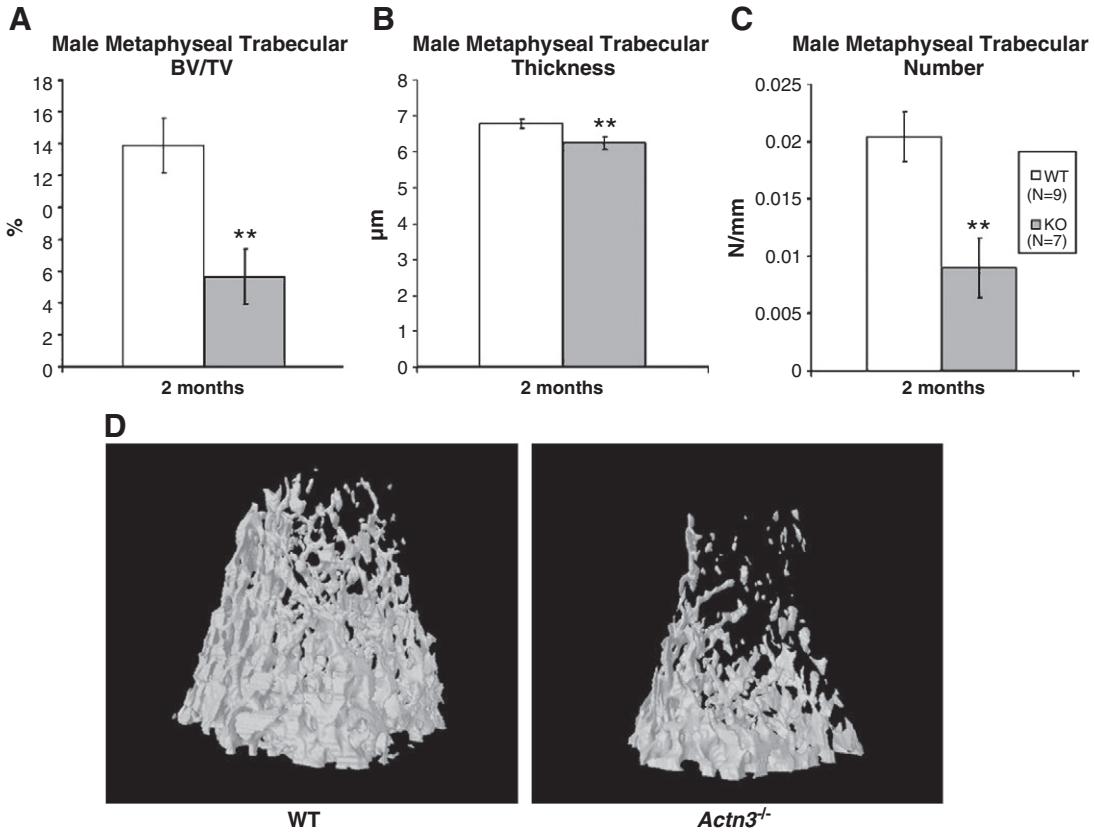

Fig. 3. Mouse metaphyseal trabecular bone architecture examined by MicroCT scan analysis (μCT). The mean ratio of trabecular bone volume *vs.* total volume (BV/TV) (3A), trabecular thickness (3B) and Trabecular Number (with 95% CI) (3C) in *Actn3*$^{-/-}$ male mice were significantly lower than that in wild-type (WT) litter mates at 2 months of age (**: $p<0.01$). Representative 3-dimensional images of trabecular bone in the metaphysis of the distal femur analysed by μCT, demonstrating the extensive reductions in bone volume and number of trabeculae in a *Actn3*$^{-/-}$ male mice (3D).

cell line, after differentiated in α-MEM containing 10% FBS. α-Actinin-3 as well as α-actinin-1 and -4 were expressed in human primary osteoblasts and mouse MC3T3-E1 pre-osteoblastic cell line, but α-actinin-2 was not present in human or mouse osteoblasts (Figs. 6A and B). We also performed PCR using cDNA synthesised from RNA isolated from differentiated murine MC3T3-E1 cells. We were able to amplify *Actn*1, *Actn*3 and *Actn*4 transcripts, but were not able to detect *Actn*2 mRNA by RT-PCR (Fig. 6C), even though the expected sized *Actn*2 fragment was generated from muscle cDNA using the same PCR primers (data not shown). Total RNA was also isolated from mouse bone marrow stromal cells and, using specific *Actn2* and *Actn3* TaqMan probes, we confirmed that *Actn*3 but not *Actn*2 is expressed in primary osteoblasts (Fig. 6D). Thus, unlike skeletal muscle, bone progenitors lack α-actinin-2 and may be unable to adequately compensate for the loss of α-actinin-3. We therefore hypothesized that the absence of α-actinin-3 may have a detrimental effect on bone quality and the *ACTN3* R577X polymorphism may be associated with variation in BMD in human populations.

α-Actinin-3 deficiency (XX-genotype) is associated with reduced BMD in older women

We genotyped two human cohorts using a previously described PCR/DdeI digestion method [18], and tested for association between R577X genotype and BMD using an analysis of covariance (ANCOVA) model, with covariates being age and body weight. The first analysed Australian Caucasian cohort for BMD association — CAIFOS (Calcium Intake Fracture Outcome Study) [34] consisted of Caucasian women over 70 years of age who had whole body BMD measurements. The distribution of genotype frequencies was consistent with the Hardy–Weinberg (HW) equilibrium law and previously published data in an Australian group of European ancestry [20] (Supplementary Table S1). In this cohort, we found that *ACTN3* R577X genotype was associated with variation in BMD ($n=733$; $p=0.003$) (Table 1). The mean values of BMD in each genotype group was in the order of RR>RX>XX (RR = 0.856; RX = 0.842; XX = 0.828), consistent with an additive genetic model. The regression model estimates that *ACTN3* R577X genotype contributes 1.1% to the variance in BMD. There is no association of R577X genotype with variations in BMI suggesting that the observed effect of *ACTN3* R577X genotype on bone mass is independent of body weight. The second Australian Caucasian cohort — DOES (the Dubbo Osteoporosis Epidemiology Study) [35] included 1061 women aged between 60 and 90 years. Again, no departure from HW equilibrium was observed for the cohort (Supplementary Table S1). There was no significant association between R577X genotypes and femoral neck bone (FnBMD), either before or after adjusting for age, body weight or body mass index.

The molecular role of α-actinin-3 in regulating bone mass

In order to understand the potential role of α-actinin-3 in the regulation of bone mass, we isolated bone marrow stromal cells from WT ($n=5$) and *Actn*3$^{-/-}$ ($n=6$) mice and studied these in cellular culture by adherence plating to tissue culture plastic. Cells were expanded and replated at a standard density (3.5×10^3 cells/cm^2) in standard differentiation medium. In order to further increase osteoblastic stimulation, duplicate wells were treated with 300 ng/ml recombinant human bone morphogenetic protein-2 (BMP2). No obvious differences were observed between WT and *Actn*3$^{-/-}$ osteoblasts in cell proliferation, differentiation, and matrix mineralisation under these conditions (Supplementary Fig. S1). However, we speculated that there may be genetic or signalling differences between

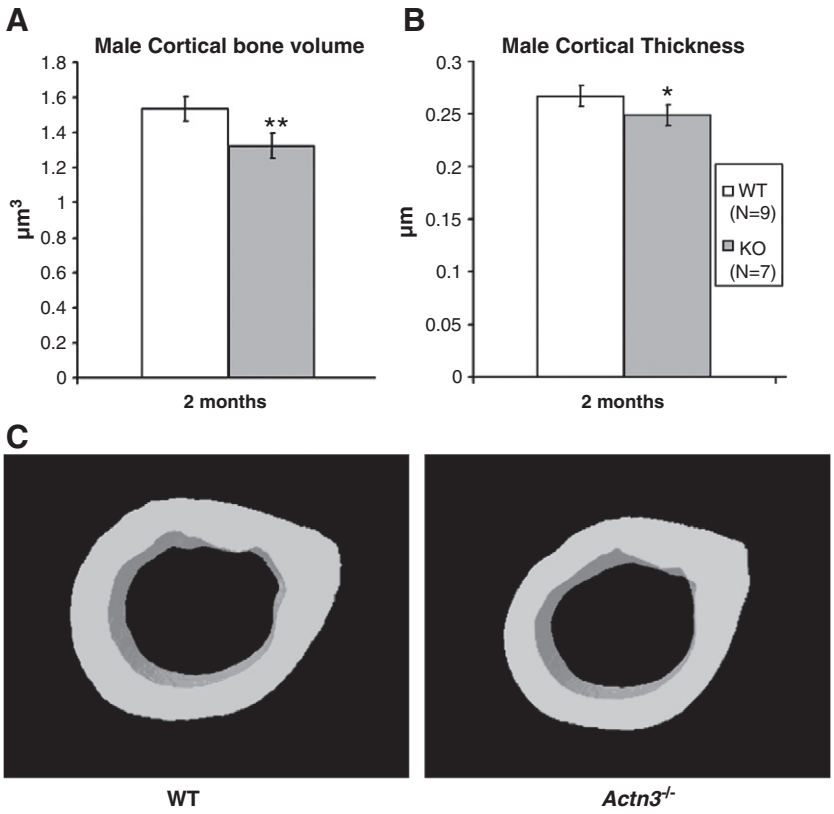

Fig. 4. Mouse diaphyseal cortical bone architecture as determined from MicroCT scan analysis (μCT). The mean cortical bone volume (4A) and thickness (with 95% CI) (4B) in *Actn3*$^{-/-}$ male mice were significantly lower than that in wild-type (WT) litter mates at 2 months of age. (**: $p<0.01$, *: $p<0.05$). Representative 3-Dimensional images of cortical bone in the diaphysis of the femur analysed by μCT, demonstrating the reductions in bone volume and thickness of the cortex in a *Actn3*$^{-/-}$ male mice (4C).

WT and *Actn3*$^{-/-}$ cells that contribute to reduced or increased osteoblastic action *in vivo*. To examine this further, we isolated total RNA from day 7 differentiated bone marrow stromal cells (WT $n=6$, *Actn3*$^{-/-}$ $n=6$) and performed microarray analysis using mouse whole-genome beadchips (Illumina). Given that the variations in BMD associated with α-actinin-3 deficiency are within the normal range, we expected limited changes in overall gene expression profiles. When all differentially expressed (DE) genes were listed using BeadStudio (Illumina), we were able to identify ~138 DE genes between WT and *Actn3*$^{-/-}$ osteoblasts with 0.2 to 5.0 fold down- or up-regulation (Supplementary Table S2). Among these, several genes have been previously shown to be associated with BMD variation and skeletal regulatory pathways. These include *Camk2d* [36], *Ctgf* [37], *Enpp1* [38], *Irs2* [39,40], *Mdm2* [41], uPA [42], *Opg* [13], *Rcan1* [43], *Sox9* [44], and *Wnt7b* [45] (Supplementary Table S3). Subsequent quantitative-PCR with TaqMan probes confirmed significant up-regulation of *Enpp1* (1.45-fold, $p=0.02$), *Wnt7b* (2-fold, $p=0.04$) and *Opg* (1.47-fold, $p=0.08$) using two-sample t-tests (Supplementary Table S3).

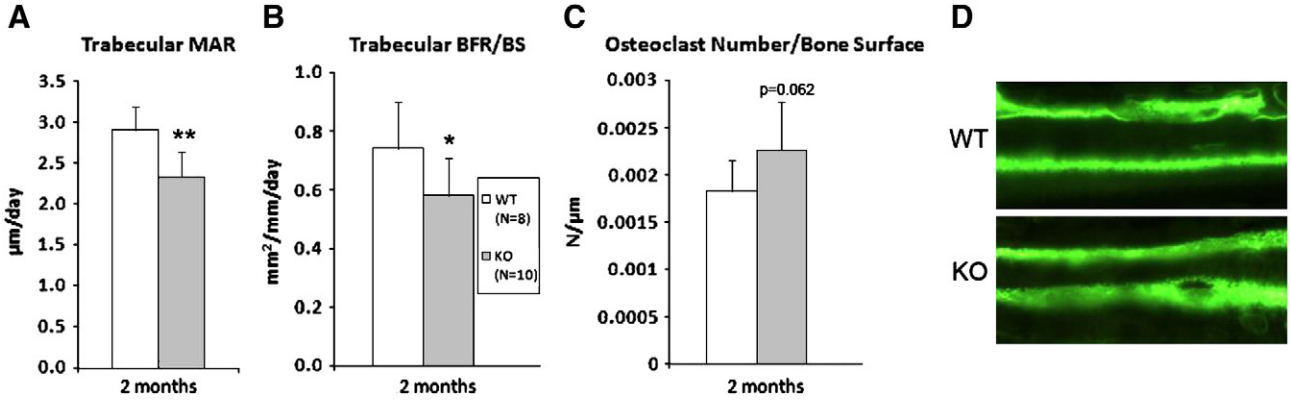

Fig. 5. Wild-type and *Actn3*$^{-/-}$ mouse bone formation and resorption parameters; Trabecular MAR (5A), Trabecular BFR/BS (5B), Trabecular OscN/BS (5C) and representative image of WT and *Actn3*$^{-/-}$ interlabel distance (5D). Bone formation and resorption parameters were examined in 2 month old Actn3 C57BL6 male WT ($n=8$) and *Actn3*$^{-/-}$ ($n=10$) mice. Mineral apposition rate (MAR) was significantly reduced (20%) in *Actn3*$^{-/-}$ mice compared to WT (**: $p<0.01$) which is also reflected in the representative trabecular bone interlabel distance of a WT and *Actn3*$^{-/-}$ mouse (D). Trabecular bone formation rate per unit bone surface (BFR/BS) was significantly reduced (21%) in *Actn3*$^{-/-}$ mice (*: $p<0.05$). *Actn3*$^{-/-}$ mice also showed a non-significant (24%, $p=0.062$) trend towards increased osteoclast number per unit bone surface in trabecular bone.

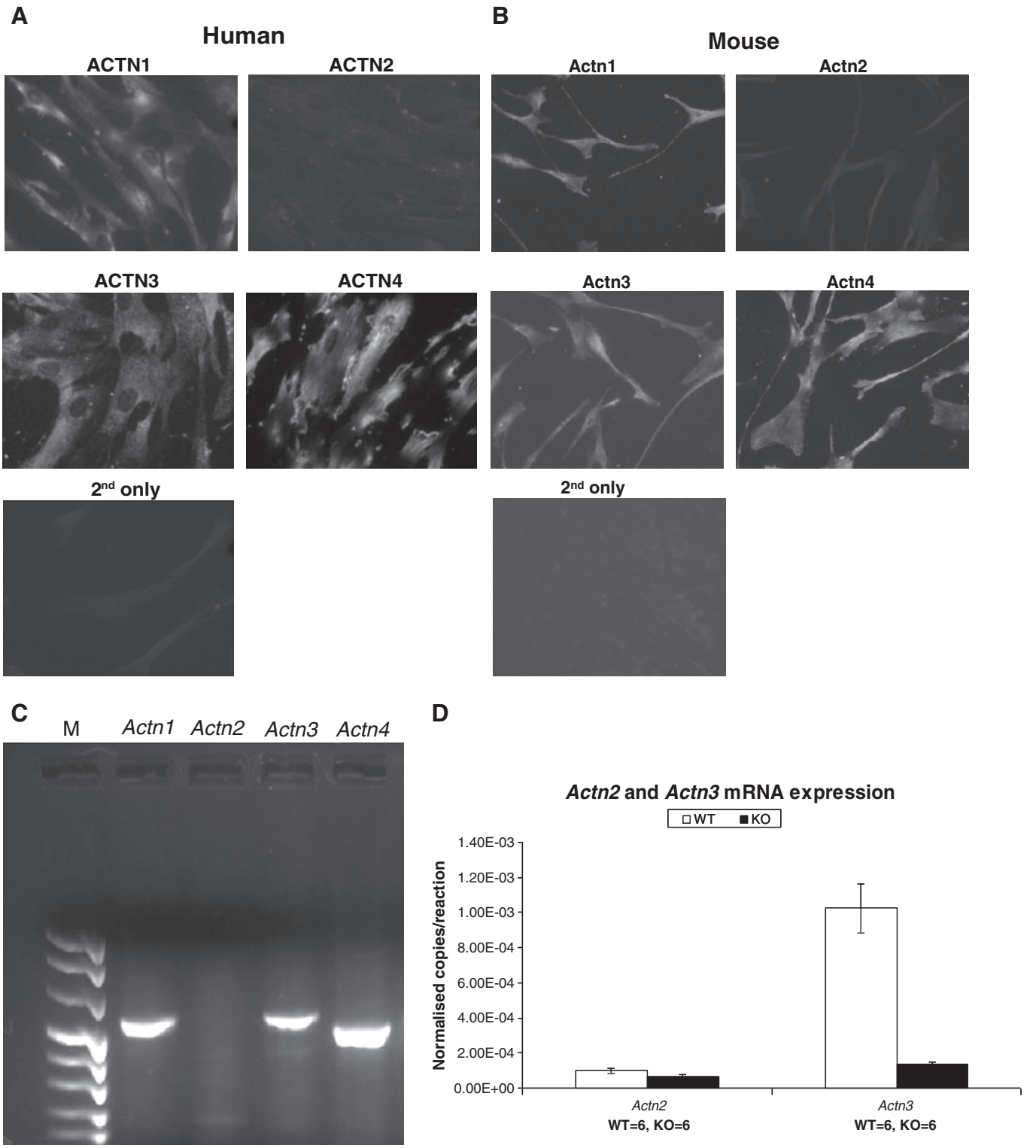

Fig. 6. Detection of expression of α-actinin-1, -2, -3 and -4 in human bone marrow stromal cells and mouse MC3T3-E1 pre-osteoblastic cell line. 6A and 6B: Immunohistochemistry (IHC) detection; Human primary bone stromal cells were isolated from a 14 year old female individual (*ACTN*3 R577X genotype RX), and cultured in differentiated medium for 6 days (6A), and mouse MC3T3 cells were cultured in differentiated medium for 4 days (6B); expression of α-actinins were detected with antibodies against α-actinin-1, -2, -3 and -4. 6C and 6D: RT-PCR (6C) and Q-PCR (6D) detection; RNA was isolated from primary mouse bone marrow stromal cells and mouse MC3T3 cells differentiated for 4 days and cDNA was synthesised with random primers; PCR was performed with primers specific to α-actinin-1, -2, -3 and -4 (6C), and Q-PCR detection was performed with TaqMan probes specific to mouse *Actn*2 and *Actn*3, normalised to the housekeeping gene Rpl35a (6D). These experiments showed that α-actinin-1, -3 and -4 are expressed in human and mouse osteoblasts, but α-actinin-2 is not expressed in osteoblasts.

Discussion

In this study, we have demonstrated that α-actinin-3 is expressed in bone, and that α-actinin-3 deficiency is significantly associated with lower bone mass in *Actn*3$^{-/-}$ mouse model. Since muscle mass (especially quadriceps muscles) in *Actn*3$^{-/-}$ mice are 16–19% less than that in WT mice [24], this could contribute to the lower bone mass in *Actn*3$^{-/-}$ mice. The difference in quadriceps muscle mass

between WT and *Actn3*$^{-/-}$ littermates is lost in male mice after 4 months of age while female mice maintain the muscle mass difference. The persistence of lower bone mass in *Actn3*$^{-/-}$ mice in all age groups and genders indicates that the lower bone mass is not solely attributable to the lower muscle mass, but may be due to an effect of α-actinin-3 deficiency on bone cells. This is supported by a 59% reduction in trabecular BV/TV. Detailed histological analysis reveal a dual mechanism for this bone loss with a 20% reduction in mineral apposition rate and a trend for a 24% increase in OscN/BS in *Actn3*$^{-/-}$ mice. Taken together these data suggest for the first time that both a reduction in osteoblast activity along with a potential increase in osteoclast activity are contributing factors for the reduced bone mass in the absence of *Actn3*. Although there were differences in the expression of genes associated with BMD in osteoblasts isolated from WT and *Actn3*$^{-/-}$ mice, this was not reflected in terms of cell differentiation, viability and growth. The discrepancy between the cell culture and mouse models suggest either the sensitivity of the cell assays were not adequate or other factors not present in our cell culture model are required in order to show these subtle differences. Analysis of mineralisation *in vivo* however suggests a mineralisation deficit, reduced MAR, not an impairment of differentiation as we saw no difference in mineralising surface. These results highlight an underlying mechanism correlating α-actinin-3 deficiency with reduced BMD. This area requires further experiments to refine our understanding of all mechanisms involved. However, our results have shown that the compensatory up-regulation of α-actinin-2 characterised in muscle does not appear to contribute as α-actinin-2 is not expressed in bone.

A novel and interesting finding of this study was the association demonstrated between *ACTN3* genotype and BMD in one out of two cohorts of elderly women studied; the positive association was independent of BMI. Since α-actinin-3 deficiency is common in the general population, its potential role as a factor influencing variations in BMD in elderly human populations warrants further study.

Our studies in skeletal muscle and bone suggest that α-actinin-3 plays a role in the regulation of tissue mass and cell size. α-Actinin-1 is known to play a role in binding the actin cytoskeleton to focal adhesions of osteoblasts [32], α-actinin-3 may also have a role in cross-linking and anchoring the actin cytoskeleton to a variety of intracellular structures and the formation of focal adhesions. Using primary osteoblast microarray we have identified up-regulation of *Enpp1*, *Opg* and *Wnt7b* in *Actn3* deficient cells. *Enpp1* is known to be a physiological inhibitor of mineralisation [46] with *Enpp1*$^{-/-}$ mice demonstrating hyper-mineralisation of bones and ectopic ossification of soft tissues [47]. Recently a human polymorphism in *ENPP1* has been associated with bone strength [38], and in mice a mutation in *Enpp1* was associated with reduced bone mass and with pathological vascular and soft tissue calcification [48]. *OPG* or osteoprotegerin is one of the key proteins in *RANK-RANKL-OPG* pathway involved in regulating osteoclast activity in bone remodelling where it acts as an antagonist to RANK-RANKL binding, thereby inhibiting osteoclast differentiation and proliferation [13,49]. *Opg* deficient mice are highly osteopenic due to excessive bone resorption [50], whereas *Opg* over expression transgenic mice show an extensive high bone mass phenotype due to a lack of osteoclastic bone resorption [51]. Furthermore, deactivating mutations in *TNFRSF11B* encoding *OPG* in humans cause systemic bone disease with low bone mass due to high bone turnover [52]. *Wnt7b* is a member of the Wnt signalling proteins that regulate mesenchymal progenitor cells differentiation into osteoblasts through the canonical Wnt/β-catenin signalling pathway [45]. Although to date *Wnt7b* expression and activity has only been shown in embryonic skeletal formation, it is clear that it also plays a role in inducing pluripotent mesenchymal cells to undergo osteoblast differentiation [53]. The precise implications of the up-regulation of *Enpp1*, *Opg* and *Wnt7b* in *Actn3*$^{-/-}$ osteoblasts is not clear, however these changes are consistent with α-actinin-3 deficiency leading to a disruption of normal mineralisation resulting in an overall decrease in bone mass. This unique investigation including both human and mouse analyses highlights an exciting and novel protein involved in osteogenesis. Deletion of α-actinin-3 is associated with low bone mass in humans and mice, with clear disruptions in mineralisation and resorption in the mouse model. Ongoing investigations to expand on the mechanisms involved will improve our understanding and potentially translate these findings into a clinical association between α-actinin-3 mutations and an increased susceptibility to low bone mass and fracture.

Acknowledgments

This project was funded in part by a grant (301950) from the Australian National Health and Medical Research Council (NHMRC).

Appendix A. Supplementary data

Supplementary data to this article can be found online at doi:10.1016/j.bone.2011.07.009.

References

[1] Kanis J, Melton III L, Christiansen C, Johnston C, Khaltaev N. The diagnosis of osteoporosis. J Bone Miner Res 1994;9:1137–41.
[2] Cummings SR, Melton LJ. Epidemiology and outcomes of osteoporotic fractures. Lancet 2002;359:1761–7.
[3] Deng HW, Chen WM, Conway T, Zhou Y, Davies KM, Stegman MR, et al. Determination of bone mineral density of the hip and spine in human pedigrees by genetic and life-style factors. Genet Epidemiol 2000;19:160–77.
[4] Ng MYM, Sham PC, Paterson AD, Chan V, Kung AWC. Effect of environmental factors and gender on the heritability of bone mineral density and bone size. Ann Hum Genet 2006;70:428–38.
[5] Recker RR, Deng H-W. Role of genetics in osteoporosis. Endocrine 2002;17:55–66.
[6] Stewart A, Reid DM. Quantitative ultrasound or clinical risk factors—which best identifies women at risk of osteoporosis? Br J Radiol 2000;73:165–71.
[7] Tabensky A, Duan Y, Edmonds J, Seeman E. The contribution of reduced peak accrual of bone and age-related bone loss to osteoporosis at the spine and hip: insights from the daughters of women with vertebral or hip fractures. J Bone Miner Res 2001;16:1101–7.
[8] Richards JB, Rivadeneira F, Inouye M, Pastinen TM, Soranzo N, Wilson SG, et al. Bone mineral density, osteoporosis, and osteoporotic fractures: a genome-wide association study. Lancet 2008;371:1505–12.
[9] Styrkarsdottir U, Halldorsson BV, Gretarsdottir S, Gudbjartsson DF, Walters GB, Ingvarsson T, et al. Multiple genetic loci for bone mineral density and fractures. N Engl J Med 2008;358:2355–65.
[10] Styrkarsdottir U, Halldorsson BV, Gretarsdottir S, Gudbjartsson DF, Walters GB, Ingvarsson T, et al. New sequence variants associated with bone mineral density. Nat Genet 2009;41:15–7.
[11] Rivadeneira F, Styrkarsdottir U, Estrada K, Halldorsson BV, Hsu Y-H, Richards JB, et al. Twenty bone-mineral-density loci identified by large-scale meta-analysis of genome-wide association studies. Nat Genet 2009;41:1199–206.
[12] Ellies DL, Viviano B, McCarthy J, Rey J-P, Itasaki N, Saunders S, et al. Bone density ligand, Sclerostin, directly interacts with LRP5 but not LRP5G171V to modulate Wnt activity. J Bone Miner Res 2006;21:1738–49.
[13] Theoleyre S, Wittrant Y, Tat SK, Fortun Y, Redini F, Heymann D. The molecular triad OPG/RANK/RANKL: involvement in the orchestration of pathophysiological bone remodeling. Cytokine Growth Factor Rev 2004;15:457–75.
[14] Richards JB, Kavvoura FK, Rivadeneira F, Styrkarsdottir U, Estrada K, Halldorsson BV, et al. Collaborative meta-analysis: associations of 150 candidate genes with osteoporosis and osteoporotic fracture. Ann Intern Med 2009;151:528–37.
[15] Blanchard A, Ohanian V, Critchley D. The structure and function of alpha-actinin. J Muscle Res Cell Motil 1989;10:280–9.
[16] Beggs AH, Byers TJ, Knoll JH, Boyce FM, Bruns GA, Kunkel LM. Cloning and characterization of two human skeletal muscle alpha-actinin genes located on chromosomes 1 and 11. J Biol Chem 1992;267:9281–8.
[17] North KN, Yang N, Wattanasirichaigoon D, Mills M, Easteal S, Beggs AH. A common nonsense mutation results in alpha-actinin-3 deficiency in the general population. Nat Genet 1999;21:353–4.
[18] Mills M, Yang N, Weinberger R, Vander Woude DL, Beggs AH, Easteal S, et al. Differential expression of the actin-binding proteins, alpha-actinin-2 and -3, in different species: implications for the evolution of functional redundancy. Hum Mol Genet 2001;10:1335–46.
[19] Yang N, MacArthur DG, Wolde B, Onywera VO, Boit MK, Lau SYM-A, et al. The ACTN3 R577X polymorphism in East and West African athletes. Med Sci Sports Exerc 2007;39:1985–8.
[20] Yang N, MacArthur DG, Gulbin JP, Hahn AG, Beggs AH, Easteal S, et al. ACTN3 genotype is associated with human elite athletic performance. Am J Hum Genet 2003;73:627–31.

[21] Moran CN, Yang N, Bailey MES, Tsiokanos A, Jamurtas A, MacArthur DG, et al. Association analysis of the ACTN3 R577X polymorphism and complex quantitative body composition and performance phenotypes in adolescent Greeks. Eur J Hum Genet 2007;15:88–93.
[22] MacArthur DG, Seto JT, Raftery JM, Quinlan KG, Huttley GA, Hook JW, et al. Loss of ACTN3 gene function alters mouse muscle metabolism and shows evidence of positive selection in humans. Nat Genet 2007;39:1261–5.
[23] Chan S, Seto JT, MacArthur DG, Yang N, North KN, Head SI. A gene for speed: contractile properties of isolated whole EDL muscle from an alpha-actinin-3 knockout mouse. Am J Physiol Cell Physiol 2008;295:C897–904.
[24] MacArthur DG, Seto JT, Chan S, Quinlan KGR, Raftery JM, Turner N, et al. An Actn3 knockout mouse provides mechanistic insights into the association between alpha-actinin-3 deficiency and human athletic performance. Hum Mol Genet 2008;17:1076–86.
[25] Quinlan KGR, Seto JT, Turner N, Vandebrouck A, Floetenmeyer M, Macarthur DG, et al. Alpha-actinin-3 deficiency results in reduced glycogen phosphorylase activity and altered calcium handling in skeletal muscle. Hum Mol Genet 2010;19: 1335–46.
[26] Walsh S, Liu D, Metter EJ, Ferrucci L, Roth SM. ACTN3 genotype is associated with muscle phenotypes in women across the adult age span. J Appl Physiol (Bethesda, Md: 1985) 2008;105:1486–91.
[27] Zempo H, Tanabe K, Murakami H, Iemitsu M, Maeda S, Kuno S. ACTN3 polymorphism affects thigh muscle area. Int J Sports Med 2010;31:138–42.
[28] Murshid SA, Kamioka H, Ishihara Y, Ando R, Sugawara Y, Takano-Yamamoto T. Actin and microtubule cytoskeletons of the processes of 3D-cultured MC3T3-E1 cells and osteocytes. J Bone Miner Metab 2007;25:151–8.
[29] Jackson WM, Jaasma MJ, Baik AD, Keaveny TM. Over-expression of alpha-actinin with a GFP fusion protein is sufficient to increase whole-cell stiffness in human osteoblasts. Ann Biomed Eng 2008;36:1605–14.
[30] Jackson WM, Jaasma MJ, Tang RY, Keaveny TM. Mechanical loading by fluid shear is sufficient to alter the cytoskeletal composition of osteoblastic cells. Am J Physiol Cell Physiol 2008;295:C1007–15.
[31] Izaguirre G, Aguirre L, Hu YP, Lee HY, Schlaepfer DD, Aneskievich BJ, et al. The cytoskeletal/non-muscle isoform of alpha-actinin is phosphorylated on its actin-binding domain by the focal adhesion kinase. J Biol Chem 2001;276:28676–85.
[32] Triplett JW, Pavalko FM. Disruption of alpha-actinin-integrin interactions at focal adhesions renders osteoblasts susceptible to apoptosis. Am J Physiol Cell Physiol 2006;291:C909–21.
[33] Seto JT, Chan S, Turner N, MacArthur DG, Raftery JM, Berman YD, et al. The effect of α-actinin-3 deficiency on muscle aging. Exp Gerontol 2011;46:292–302.
[34] Prince RL, Devine A, Dhaliwal SS, Dick IM. Effects of calcium supplementation on clinical fracture and bone structure: results of a 5-year, double-blind, placebo-controlled trial in elderly women. Arch Intern Med 2006;166:869–75.
[35] Nguyen ND, Ahlborg HG, Center JR, Eisman JA, Nguyen TV. Residual lifetime risk of fractures in women and men. J Bone Miner Res 2007;22:781–8.
[36] Sato K, Suematsu A, Nakashima T, Takemoto-Kimura S, Aoki K, Morishita Y, et al. Regulation of osteoclast differentiation and function by the CaMK-CREB pathway. Nat Med 2006;12:1410–6.
[37] Smerdel-Ramoya A, Zanotti S, Stadmeyer L, Durant D, Canalis E. Skeletal overexpression of connective tissue growth factor impairs bone formation and causes osteopenia. Endocrinology 2008;149:4374–81.
[38] Ermakov S, Toliat MR, Cohen Z, Malkin I, Altmuller J, Livshits G, et al. Association of ALPL and ENPP1 gene polymorphisms with bone strength related skeletal traits in a Chuvashian population. Bone 2010;46:1244–50.
[39] Zhou H-D, Bu Y-H, Huang Q-X, Tang L-L, Liao E-Y. Insulin receptor substrate 2 plays important roles in 17 beta -estradiol induced bone formation. Bone 2008;43:S97.
[40] Villuendas G, Botella-Carretero JI, Roldan B, Sancho J, Escobar-Morreale HF, San Millan JL. Polymorphisms in the insulin receptor substrate-1 (IRS-1) gene and the insulin receptor substrate-2 (IRS-2) gene influence glucose homeostasis and body mass index in women with polycystic ovary syndrome and non-hyperandrogenic controls. Hum Reprod (Oxford, England) 2005;20:3184–91.
[41] Salcedo A, Mayor F, Penela P. Mdm2 is involved in the ubiquitination and degradation of G-protein-coupled receptor kinase 2. EMBO J 2006;25:4752–62.
[42] DeCarlo AA, Grenett H, Park J, Balton W, Cohen J, Hardigan P. Association of gene polymorphisms for plasminogen activators with alveolar bone loss. J Periodontal Res 2007;42:305–10.
[43] Koga T, Matsui Y, Asagiri M, Kodama T, de Crombrugghe B, Nakashima K, et al. NFAT and Osterix cooperatively regulate bone formation. Nat Med 2005;11:880–5.
[44] de Crombrugghe B, Lefebvre V, Behringer RR, Bi W, Murakami S, Huang W. Transcriptional mechanisms of chondrocyte differentiation. Matrix Biol 2000;19: 389–94.
[45] Kubota T, Michigami T, Ozono K. Wnt signaling in bone metabolism. J Bone Miner Metab 2009;27:265–71.
[46] Timms AE, Zhang Y, Russell RGG, Brown MA. Genetic studies of disorders of calcium crystal deposition. Rheumatology (Oxford) 2002;41:725–9.
[47] Harmey D, Hessle L, Narisawa S, Johnson KA, Terkeltaub R, Millan JL. Concerted regulation of inorganic pyrophosphate and osteopontin by akp2, enpp 1, and ank: an integrated model of the pathogenesis of mineralization disorders. Am J Pathol 2004;164:1199–209.
[48] Babij P, Roudier M, Graves T, Han CY, Chhoa M, Li CM, et al. New variants in the Enpp 1 and Ptpn6 genes cause low BMD, crystal-related arthropathy, and vascular calcification. J Bone Miner Res 2009;24:1552–64.
[49] Murthy RK, Morrow PK, Theriault RL. Bone biology and the role of the RANK ligand pathway. Oncology (Williston Park, N Y) 2009;23:9–15.
[50] Yamazaki H, Sasaki T. Effects of osteoprotegerin administration on osteoclast differentiation and trabecular bone structure in osteoprotegerin-deficient mice. J Electron Microsc (Tokyo) 2005;54:467–77.
[51] Stolina M, Dwyer D, Ominsky MS, Corbin T, Van G, Bolon B, et al. Continuous RANKL inhibition in osteoprotegerin transgenic mice and rats suppresses bone resorption without impairing lymphorganogenesis or functional immune responses. J Immunol (Baltimore, Md : 1950) 2007;179:7497–505.
[52] Whyte MP, Mumm S. Heritable disorders of the RANKL/OPG/RANK signaling pathway. J Musculoskelet Neuronal Interact 2004;4:254–67.
[53] Hu H, Hilton MJ, Tu X, Yu K, Ornitz DM, Long F. Sequential roles of Hedgehog and Wnt signaling in osteoblast development. Development (Cambridge, England) 2005;132:49–60.